The Back Extrusion Test as a Technique for Determining the Rheological and Tribological Behaviour of Yield Stress Fluids at Low Shear Rates

Arnaud Perrot, Yannick Mélinge, Patrice Estellé, Damien Rangeard, Christophe Lanos

The back extrusion test as a technique for determining the rheological and tribological behaviour of yield stress fluids at low shear rates

Arnaud Perrot[a], Yannick Mélinge[b], Patrice Estellé[b], Damien Rangeard[b] and Christophe Lanos[b]

[a]UEB- LIMAT B, Université de Bretagne Sud, Centre de Recherche de St Maudé, 56321 LORIENT, France

[b]UEB-LGCGM, EA 3913, INSA/Université Rennes 1, France

Corresponding author: Arnaud Perrot, email: arnaud.perrot@univ-ubs.fr, tel: +33 297874577, fax: +33 297874572

Abstract:

A new method is developed to determine the rheological and tribological behaviour of viscoplastic fluids using a back extrusion test. In back extrusion geometry, the material is forced to flow in the gap between the inner and the outer cylinder. Such a flow is modelled by a Bingham constitutive law under different wall boundary conditions (stick, slip with friction and perfect slip). When steady-state flow is reached, an apparent shear rate is computed. The analysis of the inner cylinder penetration force versus the penetration depth helps us to develop a method to identify the fluid rheological and tribological properties. This method is based on an inverse analysis to identify the fluid behaviour parameters from experiments performed at different ram velocities and with different apparatus geometries. In order to study more complex fluids (Herschell-bulkley rheological behaviour, for example), an equivalent flow curve is plotted from

tests characterized by different average shear rates. The tribological behaviour is identified using different wall boundary conditions, varying the surface roughness of the cylinders. The method is applied to oil/sugar suspension and plasticine. Rheological and tribological behaviours are identified and results are compared with those obtained under steady state shear flow. The obtained rheological parameters are close to those provided by the common rheological methods (difference lower than 15%).

Résumé :

Une nouvelle méthode d'analyse rhéologique et tribologique est développée en exploitant l'écoulement de back extrusion. L'utilisation des courbes « effort d'extrusion en fonction du déplacement du cylindre intérieur » permet d'identifier les caractéristiques rhéologiques et tribologiques du fluide testé à partir des résultats de tests réalisés avec différents vitesses de pénétration du cylindre intérieur et différentes configurations géométriques. Dans le cadre de l'étude de fluides complexes incompressibles tels que les fluides d'Herschell-Bulkley frottant, la méthode permet d'aboutir à la construction d'un rhéogramme équivalent tracé à partir d'essais caractérisés par différents taux de déformation moyen. Le comportement tribologique peut être identifié en modifiant les conditions de frottement à la paroi en variant la rugosité des surfaces. La méthode est appliquée aux cas de suspensions concentrées huile/sucre et plasticine. Les comportements rhéologiques et tribologiques sont identifiés et comparés aux résultats obtenus avec la rhéométrie traditionnelle. Les paramètres rhéologiques obtenus sont proches de ceux obtenus par rhéometrie traditionnelle (différence toujours inférieure à 15%).

Keywords: Rheology, tribology, yield stress fluids, back extrusion, flow curve

Mots Clés : Rhéologie, tribologie, fluides à seuil, back extrusion, courbe d'écoulement

1 Introduction

Back extrusion, also called annular pumping, is derived from the penetrometer test. In this flow geometry, material compression induces its flow through the annulus formed between an inner cylinder and a cylindrical container. Experimental data consist in the evolution of the penetration force acting on the inner cylinder versus the displacement of the inner cylinder travel (or the time of travel). Tests are performed under constant velocity of the inner cylinder.

The back extrusion technique (BET) is often used in food engineering and is well-known as a quick, cheap test to identify the flow behaviour of complex fluids. This test configuration was first used to qualitatively estimate the ability of a fluid to flow [1-2]. As a consequence, non intrinsic parameters, such as maximum force or energy required to induce the flow, are compared to characterize the flow behaviour of complex fluids. The BET was also developed to evaluate the rheological properties of power law or Herschel-Bulkley fluids for example [3-7]. These identification methods are used to estimate the rheological properties of fluids under sticking boundary conditions. However, in those studies, the authors did not focus on the surface roughness and the risk of the material slippage at the wall, which can introduce some experimental artefacts and lead to inaccurate data analysis.

The objective of the present work is to show how the BET may be used to both estimate the rheological and tribological properties (depending on the BET cylinder surface) of yield stress fluids.

With such fluid, when rough surfaces are used, the material shear is expected at the wall. As a result, the no-slip flow material is obtained and the rheological characteristics can be studied. On the contrary, when smooth surfaces are used, slippage may occur. In such conditions, the

material may flow as a plug or may be partially sheared as in squeeze flow geometry. Consideration of wall flow properties is extremely important.

A method of data analysis is proposed and leads to build equivalent flow curves and wall friction curves from experimental data of tests performed under different conditions. The method is based on the flow properties identification of Bingham fluid parameters at a computed apparent shear rate. The considered approach consists in the modelling of the sheared material flow once steady state is reached and in computing an average shear rate when the annulus is partially and/or fully sheared. Apparent calculated Bingham parameters allow us to compute the associated shear stress value from each average shear rate value. The friction conditions can be therefore studied. Tests performed with oil/sugar suspension and plasticine illustrate our method of data analysis.

2 Flow property modelling

Let us consider the axisymmetric geometry of the BET depicted in Figure 1. The radii of the cylinder and the container are respectively denoted a and b. The squeezed yield stress fluid is assumed to be incompressible, homogeneous, inelastic, and flowing under steady-state condition.

2.1 Local and global equilibrium

Due to the axisymmetry of the BET, only the axial velocity component $V_z(r,z)$ is considered. On the basis of Bikerman's research work [8], Faure and Picart [9] define the stress profile within the gap using the stress balance equation on an annular element of material (thickness dr, height dz). This element undergoes three forces: gravity, pressure gradient and shear stress. The stress equilibrium can be written as:

$$\left[-p(z+dz)+p(z)+\rho g.dz\right].2\pi r dr=\left[(r+dr).\tau(r+dr)-r.\tau(r)\right].2\pi dz \qquad (1)$$

This relation leads to Eq. (2), which also includes gravity here, as it cannot be neglected with low yield stress material.

$$\frac{d(r\tau)}{dr} = -\psi r \qquad \text{with} \qquad \psi = -\frac{dp}{dz} + \rho g \tag{2}$$

Where p=p(z), $\tau=\tau(r)$ and ψ are respectively the pressure, the shear stress and the pressure gradient in the vertical direction (z axis). The integration of Eq. (2) according to r gives the shear stress profile $\tau(r)$ within the gap, as shown by Eq. (3). Previously cited authors showed that ψ is constant in the z direction [8].

$$\tau(r) = -\psi \frac{r}{2} + \frac{C}{r}, \qquad \text{C = constant} \tag{3}$$

Knowing the stress acting on the inner cylinder makes it possible to write the inner cylinder force balance equation. Five forces act on the inner cylinder:

- the penetration force which is recorded during the test,
- the friction force acting on the cylinder vertical surface $\pi DL\tau(a)$ where L is the penetration depth,
- the buoyancy force $\pi a^2 L\rho g$,
- the static pressure acting on the cylinder bottom surface $\pi a^2 dp/dz\rho g$,
- the force due to viscous dissipation under the penetrating cylinder Π/L where Π is the rate of energy dissipated under the inner cylinder.

Neglecting inertia forces, the force balance equation on the inner cylinder can be written[9]:

$$F = \frac{\Pi}{U} + 2\pi CL \tag{4}$$

Where F is the penetration force of the inner cylinder and U denotes the penetration velocity of the inner cylinder. The rate of energy dissipated Π can be expressed only if the velocity field under the inner cylinder is known.

The deformation of the free surface of the material is not taken into account because such

contribution can be neglected in comparison with the penetration depth L. Under the inner cylinder the flow is complex. Thus, we assume that the velocity field, as well as the viscous dissipation, remain constant during the test and only depend on the test geometry. A recent study provided by Axelesson and Gustavson has shown that for cement grout, Π/U is constant when the steady state flow is reached and can be linked to the yield stress value if U is sufficiently low [10]. As a result, the same authors have highlighted an empirical linear relationship between the penetration force and the yield stress. However, because the flow modelling seems to be very complex, we have chosen to cancel this contribution. The differentiation of Eq. (3) according to the penetration depth provides the following equation.

$$\frac{\partial F}{\partial L} = 2\pi C \qquad (5)$$

∂F/∂L is a constant. During the steady-state flow, the curve F=f(L) remains linear. C is deduced from the slope of the F(L) curve recorded during the test as shown by Figure 2.

2.2 Rheological and tribological behaviours

As previously presented, the study is mainly dedicated to the flow properties identification of viscoplastic fluids at low shear rate. The rheological behaviour of the material flowing through the BET is locally modelled from the Bingham constitutive law, as done in previous works with Couette or squeeze flow geometries [11-13]. This constitutive law presents two rheological parameters, the plastic viscosity η and the yield stress τ_0, as recalled by Eq. (5) in the case of a one dimensional flow problem. While the yield stress is not reached, the material is not sheared.

$$\tau = \left(\eta + \frac{\tau_0}{|\dot{\gamma}|} \right) \dot{\gamma} \qquad (6)$$

No slip boundary condition is of great interest for rheological measurements as it provides an easier modelling of the flow. In this case there is no need to introduce a tribological law. With

yield stress fluid, this condition is commonly achieved by using a roughened surface, manufactured at the interface of the geometries or obtained using sandpaper glued to the geometry [14-16].

In the case of smooth surfaces, slipping may occur [17-21]. This induced wall shear stress can not be sufficient to shear the material as its value can remain below the yield stress. A wall friction stress must be introduced. The Navier's law is presently used to describe the tribological behaviour of the paste at the cylinders wall. The Navier's law, used to model wall friction behaviour of highly concentrated paste using capillary tests [9], linearly links wall friction stress τ_w to the slip velocity v_{slip}.

$$\left|\tau_w\right| = \beta \left|v_{slip}\right| \qquad (7)$$

According to the value of β, different tribological behaviours may be modelled. For example, if β is equal to 0, perfect slip of the material is described., If β tends to infinity, the modelling describes a stick condition. Between these values, the modelling is able to describe a flow under slip with frictions.

Figure 3 shows that the material/wall velocity at the outer cylinder is only linked to slippage conditions while velocity at the inner cylinder interface depends on both slippage and penetration velocity.

Three different types of velocity profile in the gap between the inner cylinder and the container may occur: the first one occurs when the yield stress is reached nowhere within the gap and the material is not sheared (plug flow – Figure 3c). The second one occurs when the fluid is sheared only at the inner cylinder's surface (Figure 3b). The last one is achieved when the fluid is sheared at both wall surfaces (figure 3a). We note that slippage (i.e. plug flow) may occur in the case of smooth cylinder surfaces.

Such flow typology with both sheared and plug flow zones is similar to the one observed by MRI for extrusion flow of viscoplastic pastes [22].

2.3 Velocity and stress profiles

The combination of the stress profile obtained from the stress global equilibrium (see Eq. 2) and the Bingham constitutive law (Eq. 5) make it possible to write the stress and velocity profiles within the gap of the BET device as a function of the imposed penetration velocity of the inner cylinder U and C coefficient.

As shown in Figure 4, the flow presents three distinct zones limited by two critical radii r_1 and r_2 ($r_1 < r_2$). Here, we focus on the case with two sheared areas. Determination of the stress and velocity profiles for the case b) follows the same protocol while the case c) (plug flow) is discussed later.

Zone SF 1: between r = a and r = r_1, the material is sheared. If the yield stress is reached, the stress profile can be expressed according to the Bingham constitutive law. In this zone, the material velocity is noted $v_1(r)$ and the shear stress $\tau_1(r)$.

$$\tau_1(r) = \tau_0 + \eta.\frac{\partial v_1(r)}{\partial r} \qquad (8)$$

Zone PF: between $r = r_1$ and $r = r_2$, the yield stress is not reached and the material is submitted to plug flow. The velocity is constant and noted $v_2(r)$.

Zone SF2: Between $r = r_2$ and b, the material may be sheared due to the wall friction. If yield stress is reached, the velocity profile is deduced from the Bingham constitutive law. The velocity and the shear stress are respectively denoted $v_3(r)$ and $\tau_3(r)$.

$$\tau_3(r) = -\tau_0 + \eta.\frac{\partial v_3(r)}{\partial r} \qquad (9)$$

Eq. (3) remains valid to compute the stress profile in the gap as plotted in Figure 4.

Taking into account the Navier's law at the interfaces, the velocity profile is expressed as follows in function to radius r:

$$v_1(r) = \frac{\psi(a^2 - r^2)}{4\eta} + \frac{C}{\eta}\ln(\frac{r}{a}) + \frac{\tau_0(a-r)}{\eta} - U - \frac{\psi a}{2\beta} + \frac{C}{a\beta} \qquad \text{if } r < r_1 \qquad (10)$$

$$v_2 = v_1(r_1) = v_3(r_2) \qquad \text{if } r_1 < r < r_2 \qquad (11)$$

$$v_3(r) = \frac{\psi.(b^2 - r^2)}{4\eta} + \frac{C}{\eta}.\ln(\frac{r}{b}) + \frac{\tau_0.(r-b)}{\eta} + \frac{\psi.b}{2.\beta} - \frac{C}{b.\beta} \qquad \text{si } r > r_2 \qquad (12)$$

Four unknowns are needed to describe the flow profile in the gap: r_1, r_2, ψ and C. In order to express those parameters in terms of material behaviour parameters, four independent equations are required which are obtained from the following conditions.

(a) Yield stress reached at $r = r_1$.

$$r_1 = \frac{\tau_0 - \sqrt{\tau_0^2 + 2\psi.C}}{-\psi} \qquad (13)$$

(b) Yield stress reached at $r = r_2$.

$$r_2 = \frac{\tau_0 + \sqrt{\tau_0^2 + 2\psi.C}}{\psi} \qquad (14)$$

(c) Mass conservation.

$$\psi.\left[\frac{1}{2\beta}(a^3 + b^3) + \frac{1}{8\eta}(r_1^4 - a^4 - r_2^4 + b^4)\right] - \frac{\tau_0}{3\eta}(b^3 + a^3 - r_1^3 - r_2^3) =$$

$$C.\left[\frac{1}{\beta}(a + b) + \frac{1}{2\eta}(r_1^2 - a^2 - r_2^2 + b^2)\right] \qquad (15)$$

(d) Velocity profile continuity

$$\psi.\left[-\frac{1}{2\beta}(a + b) + \frac{1}{4\eta}(-r_1^2 + a^2 + r_2^2 - b^2)\right] = U + C.\left[-\frac{1}{\beta}(\frac{1}{a} + \frac{1}{b}) + \frac{1}{\eta}\ln(\frac{ar_2}{r_1 b})\right] + \frac{\tau 0}{\eta}(r_1 + r_2 - a - b) \qquad (16)$$

The numerical resolution of this non linear system of four equations with four unknowns allows for the entire determination of the shear stress and velocity profiles for given values of material

behaviour parameters. The mathematical resolution of the system provides a value of the C parameter which is directly linked to the force F versus L curve (Eq. 5).

3 Data analysis

3.1 Determination of the yield stress using a relaxation technique

As proposed by Osorio and Steffe [3], a simple way to determine the yield stress of material flowing through the BET consists in using the relaxation static phase of the test. The inner cylinder is stopped in the tested material after the penetration.

The penetration length has to be sufficiently long to obtain steady-state flow. Moreover, to ensure shearing, we have presently used roughened surfaces to perform relaxation tests.

Without dynamic and external solicitations, viscous forces dissipate as shown in Figure 5. After this relaxation time, the force acting on the inner cylinder remains constant and reaches a value that only depends on the yield stress and the geometry, as depicted in the Figure 5.

Then, the yield stress τ_0 is directly estimated from Eq. (17). This equation comes from the force balance equation on the inner cylinder (eq. (3)) with all time dependent terms set to zero. The relaxation phase is performed for each test.

$$F = 2\pi aL\tau_0 + \pi a^2 \rho g L \qquad (17)$$

3.2 Determination of the plastic viscosity

The plastic viscosity is determined from the experimental data obtained during the steady state penetration phase of the relaxation test (i.e. with roughened surfaces). It is deduced from the slope of the force / penetration depth curve. The procedure is the following:

- The yield stress is previously determined by the relaxation technique as detailed before.

- As a rough surface is used, this means that the material is expected to stick at the wall. So, the value of β tends to infinity.
- The only unknown parameter of the equation system (13-16) is η. The C value deduced from experiments allows us to identify the plastic viscosity from Eq. (13-16).

3.3 Flow curve identification

A geometry modification of the BET device modifies the shear rate field and the computed Bingham parameters associated to the apparent shear rate. The apparent shear rate is evaluated for each test (varying cylinders geometry and penetration variation) and the flow curve is plotted step by step. This approach presents some similarities with the one used by Estellé et al. [11-13] for the squeeze test and vane test data analysis.

An apparent shear rate is computed by means of an energy approach which consists in the balance of dissipated energy and integrates the energy dissipated at the wall and inside the material. For a non compressible dissipative material, if the dilatancy and the elasticity are neglected, a dissipation potential Γ can be introduced and expressed as follows [23]:

$$\sigma_{ij}^{(d)}.D_{ij} = 2I_2.\frac{\partial \Gamma}{\partial I_2} \quad (18)$$

where $\sigma_{ij}^{(d)}$ is the deviatoric stress tensor, $D_{ij} = 0.5\ (u_{ij}+u_{ij})$ the strain rate tensor and I_2 the second invariant of the strain rate tensor. The rate of energy dissipated in the sheared zone as a function of the dissipation potential D_e is given by Eq. (19):

$$D_e = \int_V \sigma_{ij}^{(d)}.D_{ij}.dV = \int_V 2I_2.\frac{\partial \Gamma}{\partial I_2} dV \quad (19)$$

where V is the sheared volume of the tested material ($a \leq r \leq b$). The use of the mean value theorem provides a mean value $\overline{I_2}$ that is defined by the following equation:

$$D_e = 2\left(\frac{\partial \Gamma}{\partial \sqrt{I_2}}\right)_{\sqrt{I_2}=\sqrt{\overline{I_2}}} .\sqrt{\overline{I_2}}.V \quad (20)$$

For a Bingham material, the dissipation potential Γ is:

$$\Gamma = \int \left(2\eta\sqrt{I_2} + \tau_0\right) dI_2 \quad (21)$$

The square root of $\overline{I_2}$ represents the apparent shear rate. For a one dimensional flow problem, the expression of the second invariant of the shear rate tensor is:

$$\sqrt{I_2(r)} = \dot{\gamma}(r) = \frac{\partial v_z(r)}{\partial r} \quad (22)$$

We denote $\sqrt{\overline{I_2}}$ as $\dot{\gamma}$ in the following. Then, the internal energy dissipation can be written as follow: .

$$D_e = 2.(2\eta\dot{\gamma} + \tau_0).\dot{\gamma}.V \quad (23)$$

The computation of $\dot{\gamma}$ is made using the energy balance equation.

$$D_e = F.U - \int_S v_{slip}.\tau_w dS \quad (24)$$

Where S is the contact surface between the tested material and the geometry of the BET. If we equal the global energy dissipation to the internal energy dissipation, Eq. (24) becomes:

$$2(2\eta.\dot{\gamma}^2 + \tau_0.\dot{\gamma})V = F.U - \int_S v_{slip}.\tau_w dS \quad (25)$$

The computation of Eq. (25) provides the average shear rate value. This second degree polynomial equation provides only one physically acceptable solution (i.e. positive solution). For a given shear rate, the point of the equivalent flow curve is plotted according to Bingham type fluid $\tau = \tau_0 + \eta.\dot{\gamma}$. This procedure is repeated for each test configuration in order to identify several points of the flow curve.

3.4 Determination of the tribological behaviour

The tribological behaviour is studied by performing tests with smooth surfaces in order to create slip with friction flow at the wall surface. As previously proposed under stick wall condition, tests are performed under various penetration velocities in order to build an equivalent tribological curve. Results of tests performed at different penetration velocities give different values of β that form a new tribological law. Such law provides a better description of the material tribological behaviour.

The identification of the wall friction law of the tested material is based on the curve estimation of the wall shear stress versus the average value of wall slip velocity. The slip velocity is expressed as follows:

$$v_{slip} = \frac{v_{slip}(a) + v_{slip}(b)}{2} = \frac{U + v_1(a) + v_3(b)}{2} \tag{26}$$

A step by step estimation of the β coefficient is then performed. The rheological parameter values determined for the same penetration velocity with a rough surface are introduced in a first approximation (i.e. the value of η and τ_0) in the smooth surface flow modelling. Then the β value that gives the best match between experimental and modelled penetration forces is chosen. The average shear rate is computed using Eq. (25). New rheological parameters (η, τ_0) corresponding to the computed average shear rate can be seen on the flow curve. Such data are then introduced for a second step flow modelling. This leads to a new estimation of β. This procedure is stopped when the convergence is reached (when parameter variation is less than 1% between two iterations).

If the material is not sheared in the gap (Figure 3c), the study becomes easier. This is obtained under specific experimental conditions, such as low velocity and/or large gap. This induces a plug flow and allows for a direct estimation of the material tribology. As we can easily calculate the wall shear stress and the wall slip velocity, the β parameter can be estimated. The

combination of the mass conservation equation with the continuity velocity equation provides the β parameter as a function of the slope of the F(L) curve as shown by Eq. (27).

$$\beta = \left(\frac{1}{\pi}\frac{\partial F}{\partial L} - a^2\rho g\right).\left(\frac{(b-a)(b^2-a^2)}{2Uab(b^2-ab+b^2)}\right) \quad (27)$$

4 Experimental validation

To assess the performance of flow curve recovery in BET, we have investigated the rheological and tribological properties of two materials:

- an oil and sugar dispersion
- a commercial plasticine

Tests are performed with two geometries with different rough surfaces: a smooth surface and a rough surface with asperity of 1 mm in groove and depth manufactured at the surface of the cylinders. In this configuration, diameters are 35 mm and 55 mm for the penetrating cylinder and the container, respectively. The BET was implemented on a texture analyser. It is worth noting that the compliance of the apparatus was previously measured for each geometry and velocity in order to accurately estimate the immersed length of the inner cylinder [24]. The results of the tested material in BET are compared to the ones obtained with conventional rotational shear flow data (Vane test and).

4.1 Oil - sugar suspension behaviour characteristic

Oil-sugar suspensions were prepared by mixing sucrose particles (density 1 $g.cm^{-3}$, specific surface area 0.659 m^2/cm^3, mean particle diameter 20μm) and a commercial sunflower oil. The sugar concentration was 50% in weight. The mixture was prepared at room temperature (~ 20°C) with a Hobart homogenizer. Sunflower oil was progressively added under mixing in the beaker

containing the sugar particles. A low rotation speed was initially used to avoid loose particles. Then, the rotation speed was increased and the mixing was done for 10min to finally homogenise the suspension.

Reference shear flow measurements were independently performed under isothermal condition (20°C) using a Haake Rheostress RS 100 equipped with a vane geometry and a roughened cup. This is done to circumvent the wall slip artefact. The radius of the four bladed vane geometry is 22 mm. The cup diameter is 48 mm and the gap between the cylinders is 4.2 mm. A thermostatic water bath is used to control and maintain the working temperature at 20°C. Tests are performed under up shear stress ramp and the shear flow curve is processed as done in [12, 13]. Such a method allows for plotting the flow curve of a Non-Newtonian material without any assumption on the sheared region geometry. Other work made by Yeow et al. [25] or Ancey [26] could have been used. Nguyen and Boger provide the exact expression for the rotational flow of an unbounded fluid [27]:

$$\dot{\gamma} = 2M \frac{d \ln \Omega}{d \ln M} \tag{28}$$

Where $\dot{\gamma}$ is the shear rate, M the recorded torque and Ω the rotation rate. For a given test, the shear stress is computed from the torque acting on the rotating vane:

$$\tau = \frac{M}{2\pi R^2} \tag{29}$$

Where R is the vane radius. Series of tests are peformed under constant rotational velocity at increasing or decreasing rotation rate M_j is order to use the Estellé et al. [12-13] technique. The derivation of eq. (28) is computed from values obtained during tests j and j-1. It is assumed that this average shear rate corresponds to the following shear stress which is the average value of eq. (30) from tests j and j-1.

$$\tau = \frac{M_j + M_{j-1}}{4\pi R^2} \tag{30}$$

The yield stress is also estimated at a low shear rate using the stress growth protocol of Lidell Petra and Boger [28] under a rate controlled mode. In this case, the rotation rate is set at 0.01 $rad.s^{-1}$. This velocity is in correlation with the Lidell Petra and Boger protocol and allows for an accurate determination of the yield stress (viscous effects neglected). The yield stress is also determined using Eq. (29) and M the maximum recorded torque.

Four penetration velocities ranging from 0.1 to 1 $mm.s^{-1}$ are used with the BET. For each velocity, a roughened and a smooth surface were used. As the material is biphasic, one must checked to see if it remains homogeneous, since extrusion flow may induce liquid filtration [29-31] that changes the material rheology. The measurements of initial density and density of the material located in the gap after the test show that the material remains homogeneous.

Figure 6 shows the comparison of penetration tests obtained with the different surface conditions. As expected, the two penetration curves are not superimposed. The influence of wall slip is clearly highlighted as the penetration force at a same penetration depth is lower for smooth surfaces. This proves that wall slip cannot be neglected and it represents an important experimental artefact.

Figure 7 shows that the back extrusion equivalent flow curve obtained with rough surface is in good agreement with the one obtained from the rotational vane shear flow measurement data processed with the Estellé et al. procedure. Within the range of penetration velocities used in this study, the difference in results is always under 15%. We note that the yield stress measured with the stress growth test is equal to 40.5 Pa which is in the range of the yield stress obtained with the other procedure. The tested suspension exhibits a shear-thinning Herschell-Bulckley behaviour under the condition of our work. We fit the Herschell-Bulkley law on both experimental data and obtain close values for Vane and BET as mentioned in Figure 7. The differences in fitted values are 17% for the yield stress, 9% for viscosity and 3% for flow index.

In consequence, we conclude that back extrusion is able to describe well the rheological behaviour of viscoplastic fluids

As slipping flow is obtained with the smooth surface, the tribological behaviour of the sugar dispersion can be studied. From the procedure described in section 4.2, we use the rheological parameters obtained with roughened surfaces in the data analysis of the tests performed with smooth surfaces. This makes it possible to plot a curve which links the slip velocity to the wall shear stress (Figure 8). The result shows an increase of wall shear stress with the slip velocity increasing. As the material is sheared near the wall, we note here that the computed wall shear stress τ_w is higher than the material yield stress. This means that the wall friction is sufficient to shear the material.

4.2 Plasticine

Plasticine is known to be a mainly plastic material after short compression [18]. Four tests are carried out with smooth and roughened surfaces at different inner cylinder velocities ranging from 0.1 to 1 $mm.s^{-1}$. Results are compared with shear flow measurement under constant controlled velocity obtained with a four-bladed vane of 8 mm in both height and diameter and friction measurement obtained with smooth cylinder of 8 mm in both height and diameter. This leads to independently identify the yield stress and the wall friction stress of plasticine.

BET with roughened surface tests allow to plot the equivalent flow curve. The previously proposed methods are used to study the plasticine behaviour. As expected for plastic material, the shear stress is not influenced by shear rate in the range of tested velocities (Figure 9). The back extrusion test and vane test results are also shown to be in accordance. Vane tests provide a yield stress average value of 41 kPa with the Estellé et al. procedure and 40 kPa with the stress growth test while BET provides a value of 37.5 kPa. The relative deviation is less than 5%.

With a smooth surface and at the tested penetration velocities, the material is not sheared and a plug flow appears in the gap. Eq. (24) makes it possible to compute the β parameter for a given slip velocity defined by Eq. (23). The β parameter enables the determining of a new tribological law that is reinserted into the analytical model. The results plotted in Figure 10 show that plasticine exhibits a constant wall friction stress in the range of used slip velocities (0.14 mm/s to 1.4 mm/s). Tests performed with a rotating smooth cylindrical tool confirm this value as shown by Figure 10. The rotating tool is immersed in the paste. Then, a grid is drawn on the plasticine surface to check if shearing occurs. After the test, at a constant angular velocity, the grid is checked. If the grid has not changed, we conclude that only slippage at the tool surface occurs. The tool radius and the angular velocity allow us to compute the slip velocity at the material/device interface. Those tests provide an average friction stress value of 26 kPa while BET provides a value of 25.5 kPa. Here, the relative deviation is less than 3%.

5 Conclusions

The developed back extrusion rheometer allows for behaviour characterization of highly viscous pastes in good correlation with conventional techniques. Tests performed with an oil/sugar suspension and plasticine highlight the ability of back extrusion to be used as a polyvalent tribometer/rheometer. Back extrusion tests provide a useful and simple technique to evaluate the yield stress of viscoplastic materials and to both estimate equivalent flow curve and slip velocity/ wall stress curve. The developed technique is validated using a sugar-oil suspension and plasticine. The presented results shows the ability of the BET to characterizate the rheological and tribological properties of viscoplastic fluids. Wall friction stress and yield stress values of plasticine have been estimated from back extrusion geometry. All obtained values are in agreement with the values obtained by conventional measurements.

References

[1] Lee SY: Relating descriptive analysis and instrumental texture data of proceeded diced tomatoes, Food Quality and Preference 10 (1999) 447-455.

[2] Brusewitz GH, Yu H: Back extrusion method for determining properties of mustard slurry, J. Food Sci. and Techn. 27 (1996) 259-265.

[3] Osorio FA, Steffe JF: Evaluating H-B fluids with the back extrusion technique, Rheol. Acta. 23 (1997) 213-220.

[4] Gurjal HS, Sodhi NS: Back extrusion of wheat porridge, J. Food Eng. 52 (2002) 53-56 .

[5] Picart D: A penetroviscometer for Newtonian and viscoplastic fluids. Instr.Sc.Techn., 29 (2001) 169-184.

[6] Basner T, Pehlke R, Sachdev A, Thin-wall back extrusion of partially remelted semi-solid Sn-Pb, Mettalurgical and materials transactions A. 31 (2000) 57-62.

[7] Vieira EA, Ferrante M, Prediction of rheological behaviour and segregation susceptibility of semi-solid aluminium silicon alloys by a simple back extrusion test, Acta Materiala (2005), 5379-5386.

[8] Bikerman JJ: A penetrometer for very viscous liquids, J. Colloid Sci. 3 (1947) 75-85.

[9] Faure JP, Picart D: Rheological behaviour of paste explosive material, 30th annual conference of ICT, Karlsruhe Germany (1999).

[10] Axelsson M, Gustafson G: A robust method to determine the shear strength of cement-based injection grouts in the field, Tunnelling and Underground Space Technology 21(2006), 499-503.

[11] Estellé P, Lanos C, Toutou Z, Servais C: Squeeze flow of sticking viscoplastic fluids: Direct identification of behaviour parameters by an equivalent flow curve, 16th International Congress on Rheology, Seoul, (2004).

[12] Estellé P, Lanos C, Perrot A: Processing the Couette viscometry data using a Bingham approximation in shear rate calculation, Journal of Non-Newtonian Fluid Mechanics 154 (2008) 31-38.

[13] Estellé P, Perrot A, Lanos C, Amziane S: Processing the vane shear flow data from Couette analogy, Applied Rheology 18 (2008) 34-43.

[14] Roussel N, Lanos C: Plastic fluid flow parameters identification using a simple squeezing test, Applied Rheology 13 (2003) 132-141.

[15] Toutou Z., Roussel N Lanos C: The squeezing test, a tool to identify firm cement based material's rheological behaviour and evaluate their extrusion ability, Cement and Concrete Research 35 (2005) 1891-1899.

[16] Tchamba JC , Amziane S, Ovarlez G and Roussel N: Lateral stress exerted by fresh cement paste on formwork : laboratory experiments, Cement and Concrete Research **38** (2008) 459–466.

[17] Saak AW, Jennings HM and Shah SP: The influence of wall slip on yield stress and visco-elastic measurements of cement pastes, Cem. Concr. Res. **31** (2001) 205–212.

[18] Estellé P, Lanos C, Perrot A, Servais C: Slipping zone location in squeeze flow, Rheologica Acta, 45 (2008) 444-448.

[19] Barnes HA: A review of the slip (wall depletion) of polymer solutions, emulsions and particle suspensions in viscometers: its cause, character and cure. J Non-Newton Fluid Mech 56 (1995) 221–251.

[20] Tang HS, Kalyon DM: Estimation of the parameters of Herschel-Bulkley fluid under wall slip using a combination of capillary and squeeze flow viscosimeters. Rheologica Acta 43 (2004) 80-88.

[21] Meeten GH: Effects of plate roughness in squeeze flow rheometry, Journal of Non-Newtonian fluids mechanics 124 (2004) 51-60.

[22] Rabideau BD, Moucheront P, Bertrand F, Rodts S, Roussel N, Lanos C and Coussot P: The extrusion of a model yield stress fluid imaged by MRI velocimetry Journal of Non-Newtonian fluids mechanics 165 (2010) 393-408.

[23] Germain P., Mécanique, tome II, 381, Ellipses (1986)

[24] Estellé P, Lanos C, Mélinge Y, Servais C: On the optimisation of a texture analyser in squeeze flow geometry, Measurement 39 (2006) 771-777.

[25] Yeow YL, Woan CK, Pannie PPT, Solving the inverse problem of Couette viscometry y Tikhonov regularization, J. Rheol. 44 (2000) 1335–1351.

[26] C. Ancey, Solving the Couette inverse problem using a wavelet-vaguelette decomposition, J. Rheol. 49 (2) (2005) 441–460.

[27] Nguyen QD, Boger DV: Characterization of yield stress fluids with concentric cylinder viscometers, Rheol. Acta 26 (1987) 508–515.

[28] Liddell PV, Boger DV, Yield stress measurements with the vane, J. Non-Newtonian Fluid Mech. 63 (1996) 235-261.

[29] Perrot A, Rangeard D, Mélinge Y, Estellé Y, Lanos C: Extrusion criterion for firm cement based materials, Applied Rheology 19 (5) (2009) 53042.

[30] Yu AB , Burbidge AS, Bridgwater J, Saracevic Z: Liquid maldistribution in particulate paste extrusion, Powder Tech. 103 (1999) 103-109.

[31] Burbidge AS, Bridgwater J, Saracevic Z: Liquid migration in paste extrusion, Chem. Eng. Res. Design 73 (1995) 810-816.

Figure captions

Figure 1: Schematic view of the back extrusion geometry

Figure 2: Determination of the coefficient C from the force versus immersed length curve.

Figure 3: Back extrusion velocity profile scenario and wall friction stresses for yield stress fluid – relationship between slip velocity and friction stress. a) material is sheared at both cylinder interfaces - b) material is sheared only at the inner cylinder interface – c) material is not sheared.

Figure 4: Stress profile in the gap – illustration of the shearing conditions in zone A and C

Figure 5: yield stress value determination by a relaxation technique

Figure 6: Comparison of the penetration curves of sugar dispersion obtained with BET geometry with smooth and rough surfaces (0.5 $mm.s^{-1}$ penetration velocity).

Figure 7: Comparison of the flow curves of sugar dispersion obtained from vane test measurement and BET under stick condition (roughened surfaces).

Figure 8: tribological curve of the oil-sugar dispersion . Back extrusion test results using smooth surfaces

Figure 9: Plastic behaviour of plasticine described by vane tests and back extrusion tests

Figure 10: Tribological behaviour of plasticine described by vane tests and back extrusion tests

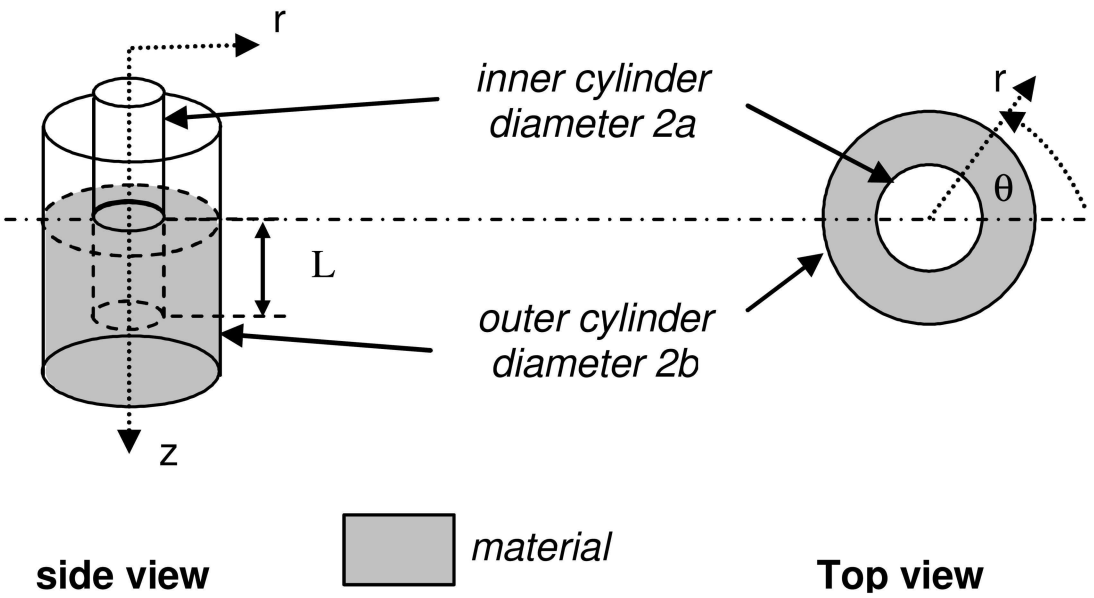

Figure 1

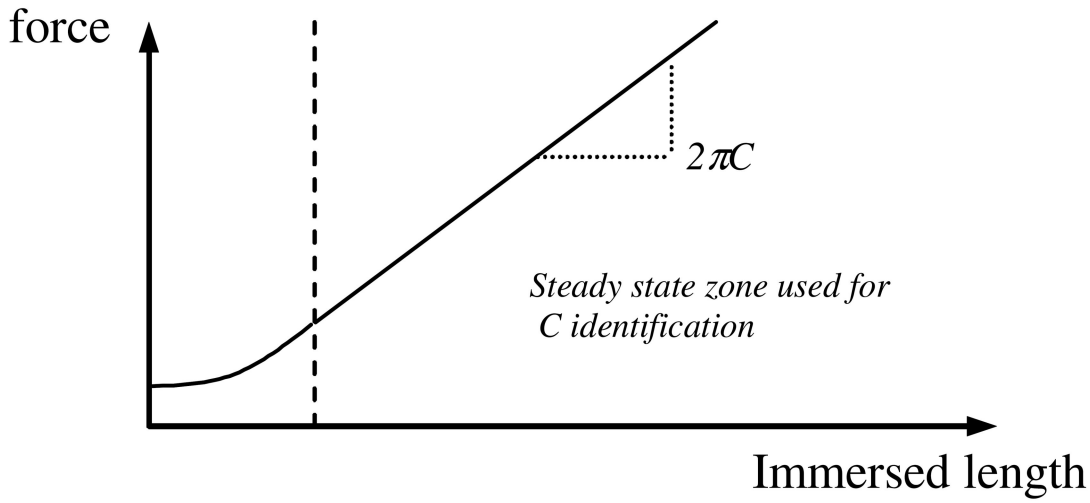

Figure 2

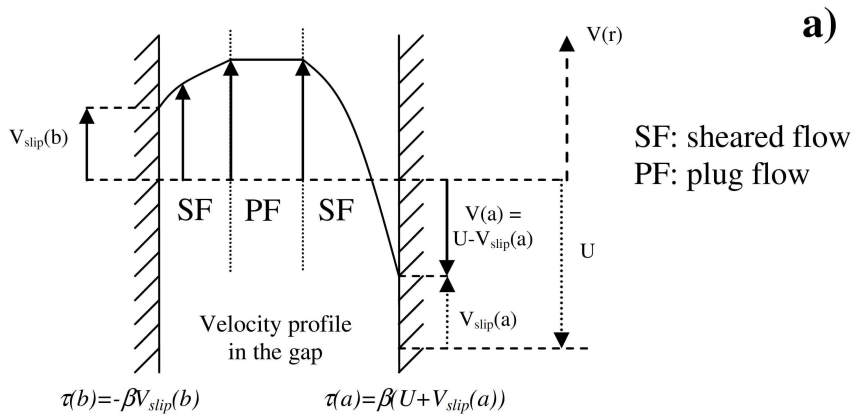
a)
V(r)
$V_{slip}(b)$
SF
PF
SF
V(a) =
$U-V_{slip}(a)$
U
$V_{slip}(a)$
Velocity profile
in the gap
$\tau(b)=-\beta V_{slip}(b)$
$\tau(a)=\beta(U+V_{slip}(a))$
SF: sheared flow
PF: plug flow

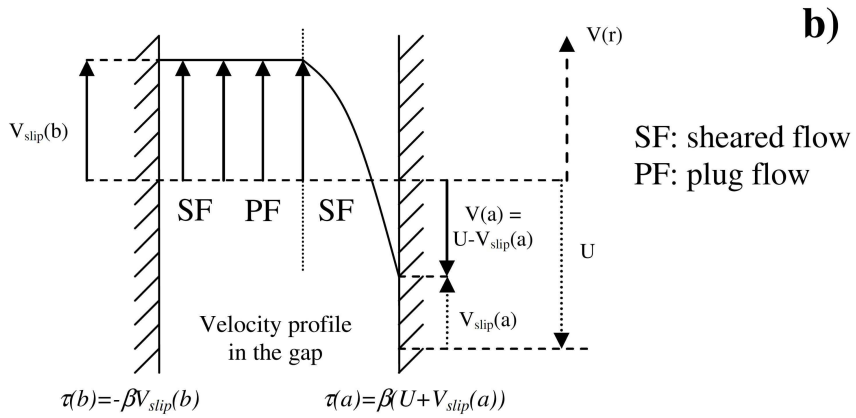
b)
V(r)
$V_{slip}(b)$
SF
PF
SF
V(a) =
$U-V_{slip}(a)$
U
$V_{slip}(a)$
Velocity profile
in the gap
$\tau(b)=-\beta V_{slip}(b)$
$\tau(a)=\beta(U+V_{slip}(a))$
SF: sheared flow
PF: plug flow

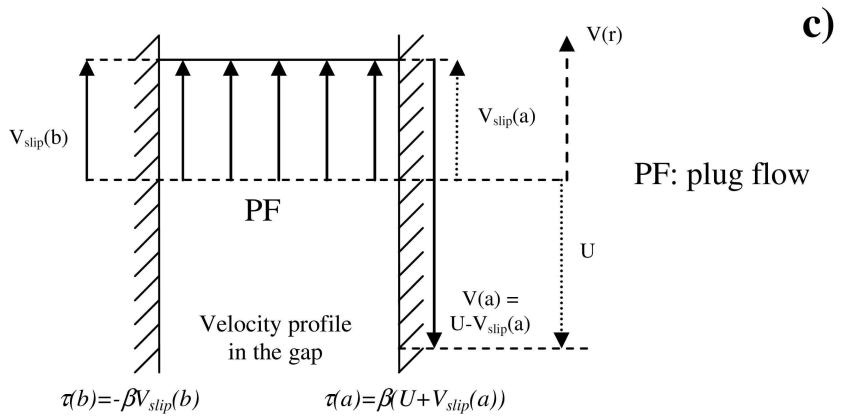
c)
V(r)
$V_{slip}(b)$
$V_{slip}(a)$
PF
U
V(a) =
$U-V_{slip}(a)$
Velocity profile
in the gap
$\tau(b)=-\beta V_{slip}(b)$
$\tau(a)=\beta(U+V_{slip}(a))$
PF: plug flow

Figure 3

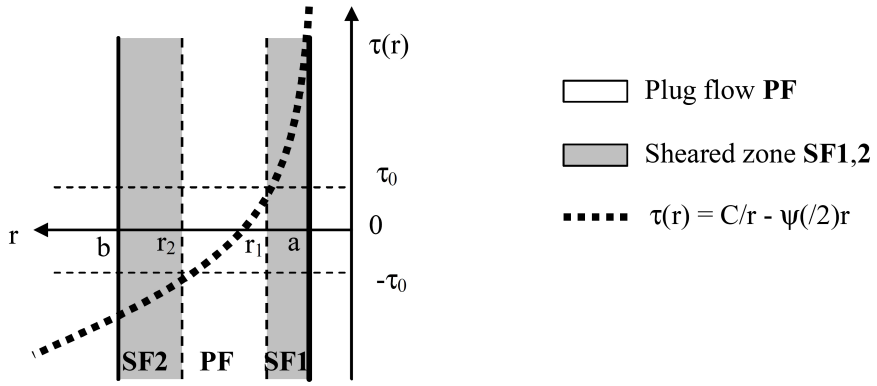

Figure 4

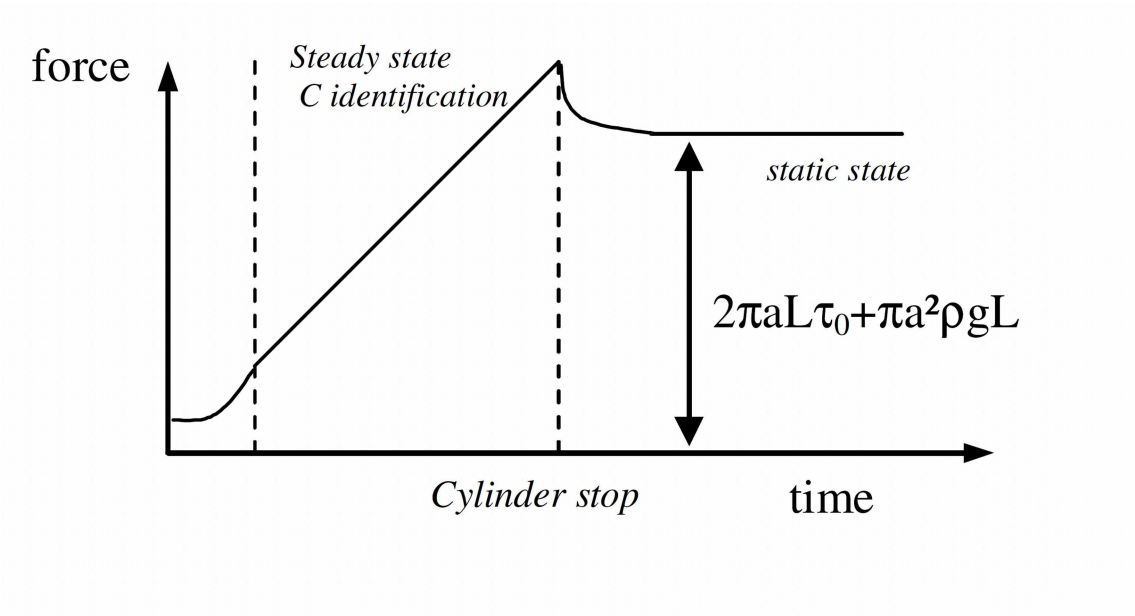

Figure 5

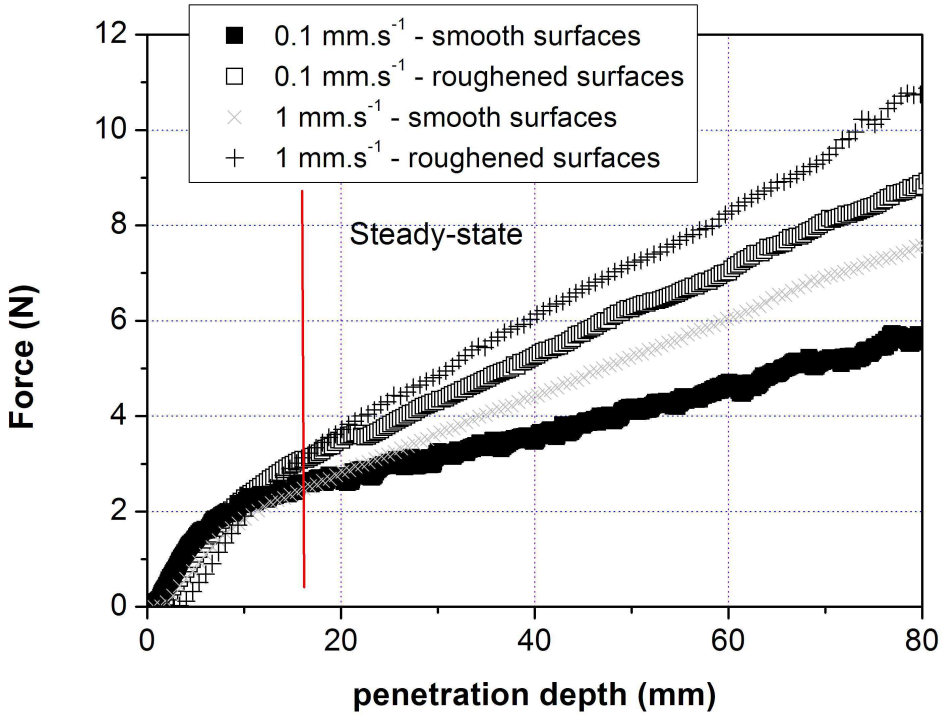

Figure 6

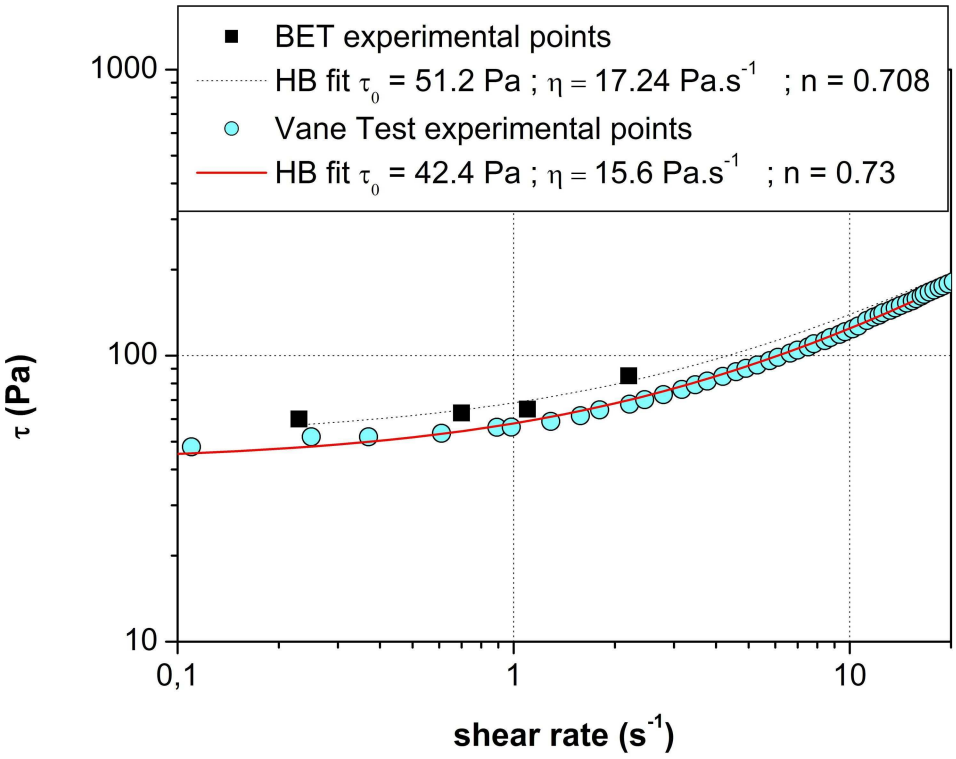

Figure 7

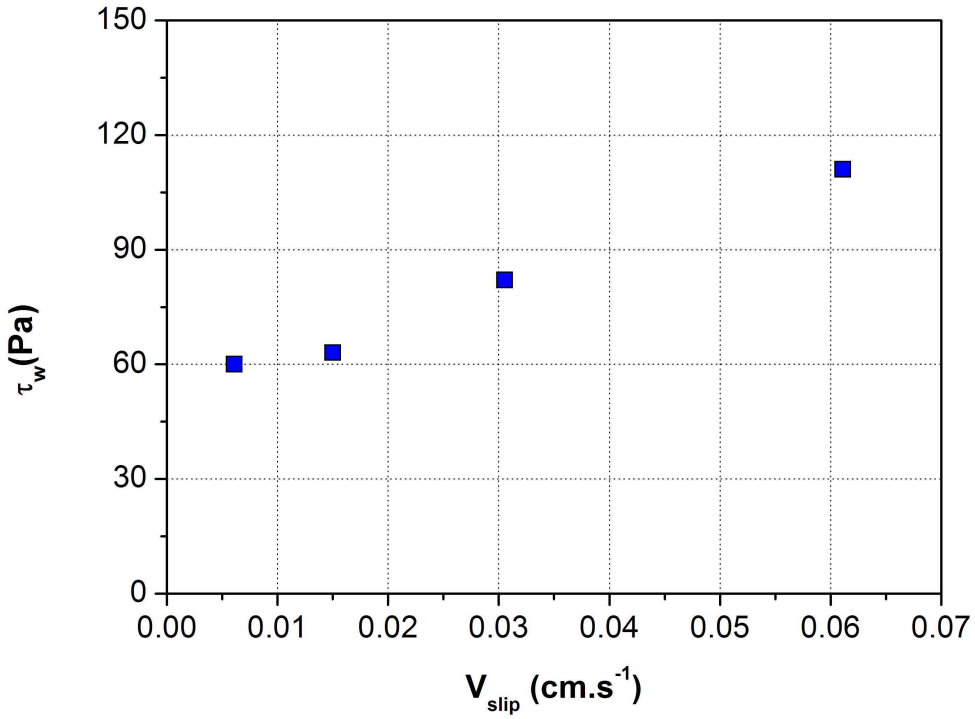
150
120
90
60
30
0
τ_w(Pa)
0.00
0.01
0.02
0.03
0.04
0.05
0.06
0.07
V_{slip} (cm.s^{-1})

Figure 8

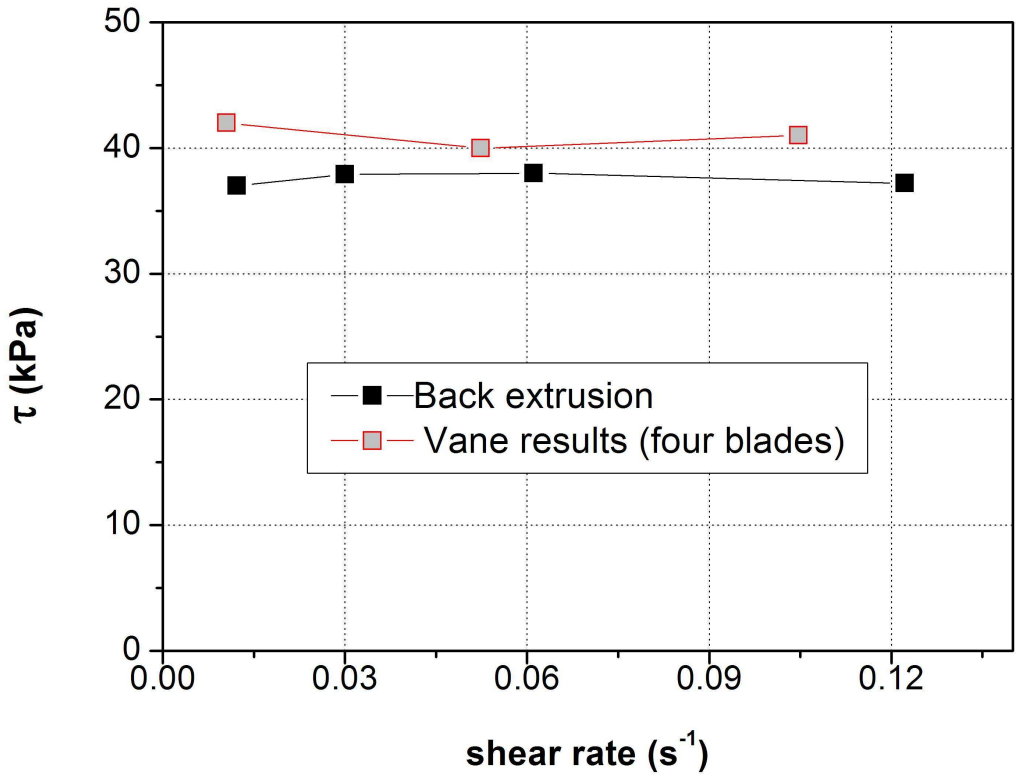
50
40
30
20
10
0
τ (kPa)
0.00
0.03
0.06
0.09
0.12
shear rate (s^{-1})
Back extrusion
Vane results (four blades)

Figure 9

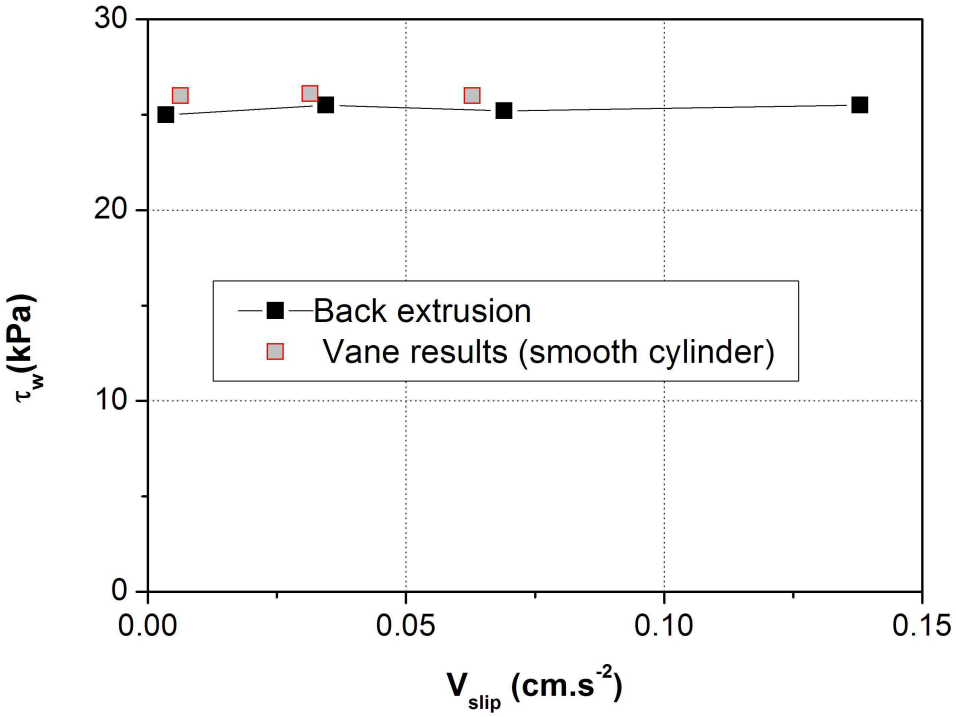

Figure 10